Phenothiazine-Carbazole-based Bis Oxime Esters (PCBOEs) for Visible Light Polymerization

Zheng Liu, Bin Song, Yijun Zhang, Céline Dietlin, Fabrice Morlet-Savary, Michael Schmitt, Didier Gigmes, Frédéric Dumur, Jacques Lalevée

Phenothiazine-Carbazole-based Bis Oxime Esters (PCBOEs) for Visible Light Polymerization

Zheng Liu[‡1], Bin Song[‡2], Yijun Zhang[2], Céline Dietlin[2], Fabrice Morlet-Savary[2], Michael Schmitt[2], Didier Gigmes[1], Frédéric Dumur*[1] and Jacques Lalevée*[2]

1 Aix Marseille Univ, CNRS, ICR UMR 7273, F-13397 Marseille, France

2 Université de Haute-Alsace, CNRS, IS2M UMR 7361, F-68100 Mulhouse, France

*Corresponding authors: frederic.dumur@univ-amu.fr; jacques.lalevee@uha.fr

[‡] The two first authors equally contributed this work

Abstract

In this study, a series of seven PCBOEs was innovatively designed and successfully synthesized for the first time by bridging a phenothiazine and a carbazole unit by mean of an acetylene spacer and bearing oxime ester groups as end groups on both sides. Structures of the different difunctional oxime esters were confirmed through NMR and HRMS. All PCBOEs exhibited excellent light absorption properties in the visible range. Upon excitation with a 405 nm LED for 60 s, a complete photolysis of oxime esters could be achieved. Parameters such as the singlet state energy and the triplet state energy demonstrated the facile generation of the corresponding radicals upon light absorption by PCBOEs. Photopolymerization kinetics in TMPTA confirmed the homolytic cleavage of oxime esters and the generation of radicals. CO_2 absorption peaks were detected when the PCBOEs/TMPTA systems were excited with a 405 nm LED. Based on the positive results, the photochemical mechanisms of polymerization with PCBOEs was proposed. PCBOE3 was identified as the best candidate of the series and this bifunctional oxime ester was successfully used for the 3D-printing of the "IS2M" logo via DLW. Experimental results from DSC also confirmed that PCBOEs not only serve as photoinitiators but also possess high reactivity as thermal initiators.

1. Introduction

Acrylate-based photopolymerization processes play a pivotal role in the development of advanced materials and technologies across various industries including coatings[1], adhesives[2], biomedical materials[3], holography[4, 5] and 3D printing[6]. The pursuit of environmentally friendly and energy-efficient polymerization methods has led to an increasing interest in visible light photopolymerization, avoiding the use of harmful UV radiation.[7-10] So, the design and exploration of novel photoinitiators containing oxime esters (OXEs), known for their abilities to undergo a rapid photolysis under visible light and to generate highly reactive free radicals have emerged as a key research focus in recent years.[11-14]

Phenothiazine-based OXEs are ideal candidates for initiating light-induced polymerization reactions due to their broad absorption spectra, compatibility with various monomers, excellent stability upon storage and easy of synthesis.[10] Additionally, contrarily to a related structure i.e. carbazole which is extensively studied for the design of photoinitiators, phenothiazine already absorb in the visible range even when unsubstituted contrarily to carbazole that exhibit a UV-centered absorption. In 2023, Noon et al. utilized two photoinitiators, PTZ2 and PTZ3, comprising a phenothiazine unit as the chromophore and an oxime ester moiety as the photocleavable group (see Scheme 1). These two structures could efficiently initiate the free radical polymerization (FRP) of di(trimethylolpropane)tetraacrylate (TA) upon excitation with a 405 nm LED at an intensity of 110 mW · cm^{-2}.[15] After 140 s of irradiation, PTZ3 (1 wt%) achieved the highest final conversion, reaching up 81%. In 2023, Zhang et al. synthesized thirteen nitro-substituted phenothiazine-based OXEs with various substituents (A-M) (See Scheme 1).[16] After 300 s of irradiation with a 405 nm LED at an intensity of 110 mW · cm^{-2}, the highest final conversion for the initiation of trimethylolpropane triacrylate (TMPTA) by OXE-A (1×10^{-5} mol · g^{-1}) reached 64%. In 2023, Zhang et al. successfully synthesized twelve phenothiazine derivatives containing *bis* oxime esters (OXE-A1 - OXE-B9) that could generate twice more free radicals per molecule due to the double functionality upon irradiation (see Scheme 1).[17] After exposure to a 405 nm LED at an intensity of 110 mW · cm^{-2} for 800 s, OXE-A1 (1×10^{-5} mol · g^{-1}) achieved the highest conversion during the FRP of TMPTA,

reaching 80%.

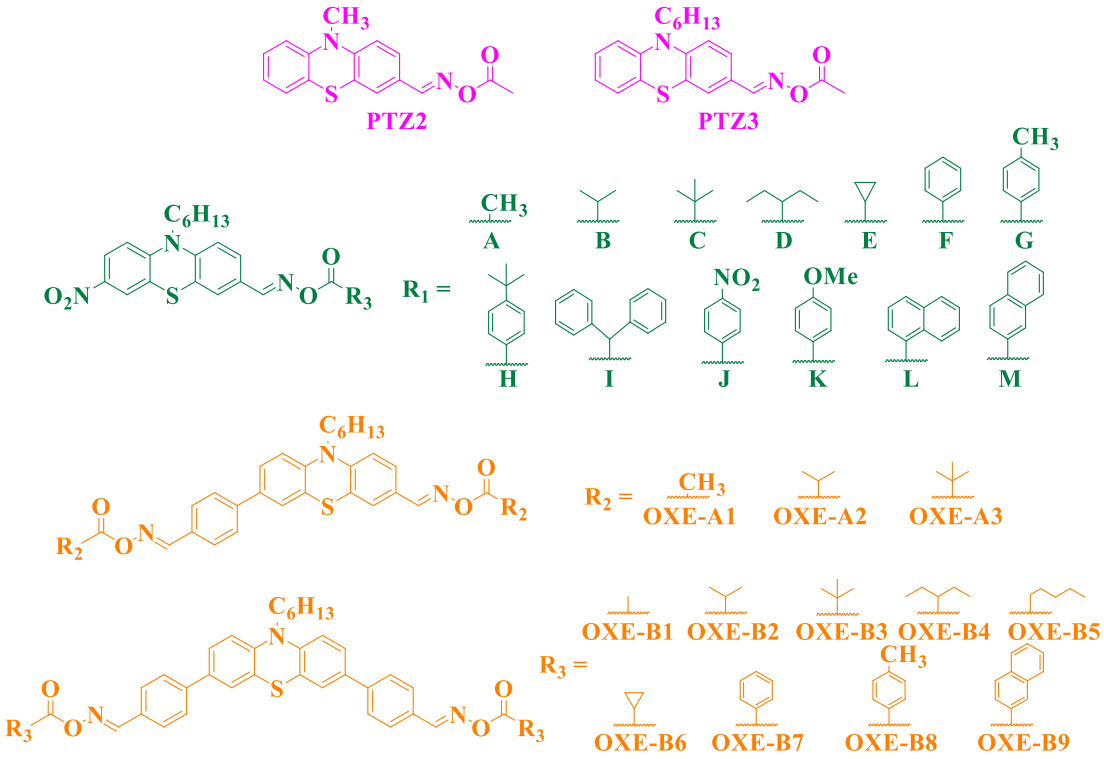

Scheme 1. Structures of reported phenothiazine-based OXEs

The popularity of carbazole to design OXEs stem from its excellent light absorption characteristics, photostability, high reactivity upon light excitation and ease of modification of its scaffold.[14, 18] The carbazole/oxime ester combination has been extensively studied for the design of Type I photoinitiators and concerning oxime esters, carbazole was undoubtedly the most extensively studied scaffold, with more than 100 reported structures.[14, 19-25] The part of reported carbazole-based OXEs (OXE-M, 3, C9, B3 - B8), known for their excellent photoinitiating performance, are shown in Scheme 2. The final conversions of these OXEs obtained during the polymerization of TA and TMPTA after exposure to 405 nm LED at an intensity of 110 mW · cm^{-2} radiation were higher than 68%. Among them, the final conversions obtained with compound 3 and C9 (0.5 wt%) during the FRP of TMPTA exceeded 80% after continuous irradiation with a 405 nm LED at an intensity of 110 mW · cm^{-2} for 400 s and 600 s, respectively.

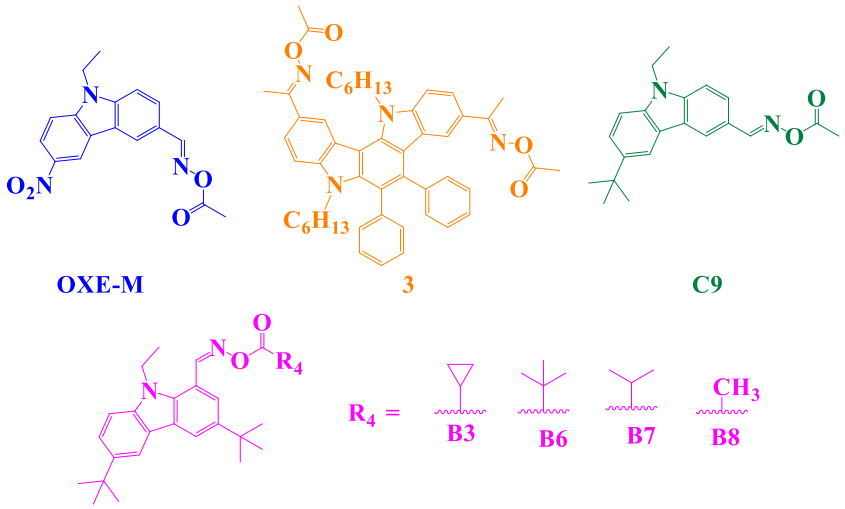

Scheme 2. A few examples of structures reported in the literature for carbazole-based OXEs

Considering that phenothiazine and carbazole are excellent scaffolds for the design of OXEs, their combination and their covalent linkage by mean of a π-conjugated spacer that could enable an efficient electronic delocalization between the two moieties is of interest. By employing an acetylene group as a π-conjugated spacer to covalently link phenothiazine to carbazole, a novel chromophore of extended π-conjugation could be produced.[26-28] Choice of an acetylene group over an ethylene group is also justified by the higher solubility this spacer can provide to the overall assembly. The solubilizing effect of the acetylene group over the ethylene one is well-documented in the literature.[29-31] To date, use of this strategy to design Type I photoinitiator of photopolymerization has only been reported once in the literature. In 2017, Ma et al. successfully synthesized one oxime ester based on phenothiazine, linked to a carbazole moiety by mean of an ethynyl bridge (PTZ-OXE-2) (see Scheme 3).[32] After 30 s of irradiation with a 405 nm light source, the final conversion for the initiation of Tripropylene glycol diacrylate (TPGDA) at a concentration of 1 wt% was 85%. However, the application of the mentioned OXEs in the photopolymerization of TMPTA has not been explored yet. Additionally, no difunctional oxime esters resulting from the phenothiazine/carbazole combination have been reported yet in the literature.

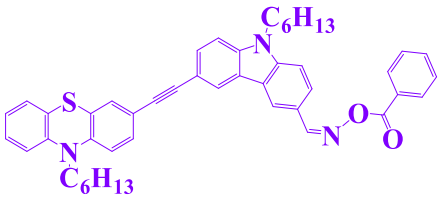

Scheme 3. Structures of reported phenothiazine-carbazole-based OXEs PTX-OXE-2

Based on the aforementioned facts, this study wants to connect phenothiazine and carbazole by mean of an acetylene spacer and introduces two oxime ester moieties on both sides of the dye backbone in order to obtain difunctional OXEs for the free radical polymerization of acrylates. According to existing literature, alkyl radicals produced from the cleavage of oxime esters exhibit a higher reactivity than aryl radicals.[11, 13, 14] Moreover, oxime esters containing alkyl groups have shown superior final conversions in initiating the polymerization of TMPTA compared to their aryl counterparts. Therefore, the PCBOEs examined in this study exclusively contain alkyl groups. PCBOEs were successfully synthesized, and their molecular structures were confirmed through nuclear magnetic resonance (NMR), as well as high-resolution mass spectrometry (HRMS). UV-visible absorption spectra were employed to characterize their light absorption properties and their photocleavage during irradiation (photolysis experiments). Parameters such as singlet state energy, triplet state energy and N-O bond dissociation energy (BDE) were utilized for investigating their individual properties. Theoretical calculations, electron spin resonance (ESR) and analysis of the Fourier Transform Infrared Spectroscopy (FTIR) spectra enabled to understand the photopolymerization mechanism involved with these PCBOEs. Photopolymerization kinetics obtained with a 405 nm LED were characterized using FTIR. Combining the experimental results, the photoinitiation mechanism with PCBOEs could be proposed. Direct laser write (DLW) was employed to 3D print designed patterns using selected PCBOEs with high photopolymerization kinetics under a 405 nm LED light source. Additionally, the thermal initiation properties of the selected PCBOEs for the FRP of TMPTA was examined using differential scanning calorimetry (DSC).

2. Results and discussion

2.1 Synthesis of the dyes

The detailed synthetic steps for producing PCBOEs are illustrated in Scheme 4. A convergent approach was used for the synthesis of PCBOEs. Thus, the introduction of the iodine group at the sixth position of phenothiazine was achieved in 92% and yielded C1 starting from 9-hexyl-9*H*-carbazole-3-carbaldehyde C0 using oxidative conditions (KIO_3 and KI). Subsequently, a trimethylsilyl group could be introduced on 9-hexyl-6-iodo-9*H*-carbazole-3-carbaldehyde C1 by mean of a Sonogashira cross-coupling reaction using ethynyltrimethylsilane, $Pd(PPh_3)_2Cl_2$ as the catalyst and triethylamine as the base. The desired product C2, 6-ethynyl-9-hexyl-9*H*-carbazole-3-carbaldehyde, was successfully obtained in 87% yield after hydrolysis of the silyl group with K_2CO_3.

Parallel to this, 10-hexyl-10*H*-phenothiazine-3-carbaldehyde P1 was first prepared in 78% yield by mean of a Vilsmeier-Haack reaction. Subsequently, reaction of P1 with *N*-iodosuccinimide yielded 10-hexyl-7-iodo-10*H*-phenothiazine-3- carbaldehyde 5-oxide P2 in 21% yield. The two carbazole and phenothiazine products (P2 and C2) were then connected by a Sonogashira reaction in 87% yield, producing PC1. PCBOE0 was obtained by introducing the oxime group through the condensation of hydroxylamine on the aldehyde group, what could be achieved in 97% yield. PCBOE1-PCBOE7 were individually obtained with yields ranging from 72% to 91% by esterification with the appropriate acyl chloride using triethylamine as the base. The structures of all intermediate products were confirmed by NMR and HRMS, with detailed results provided in the Supplementary Information (SI).

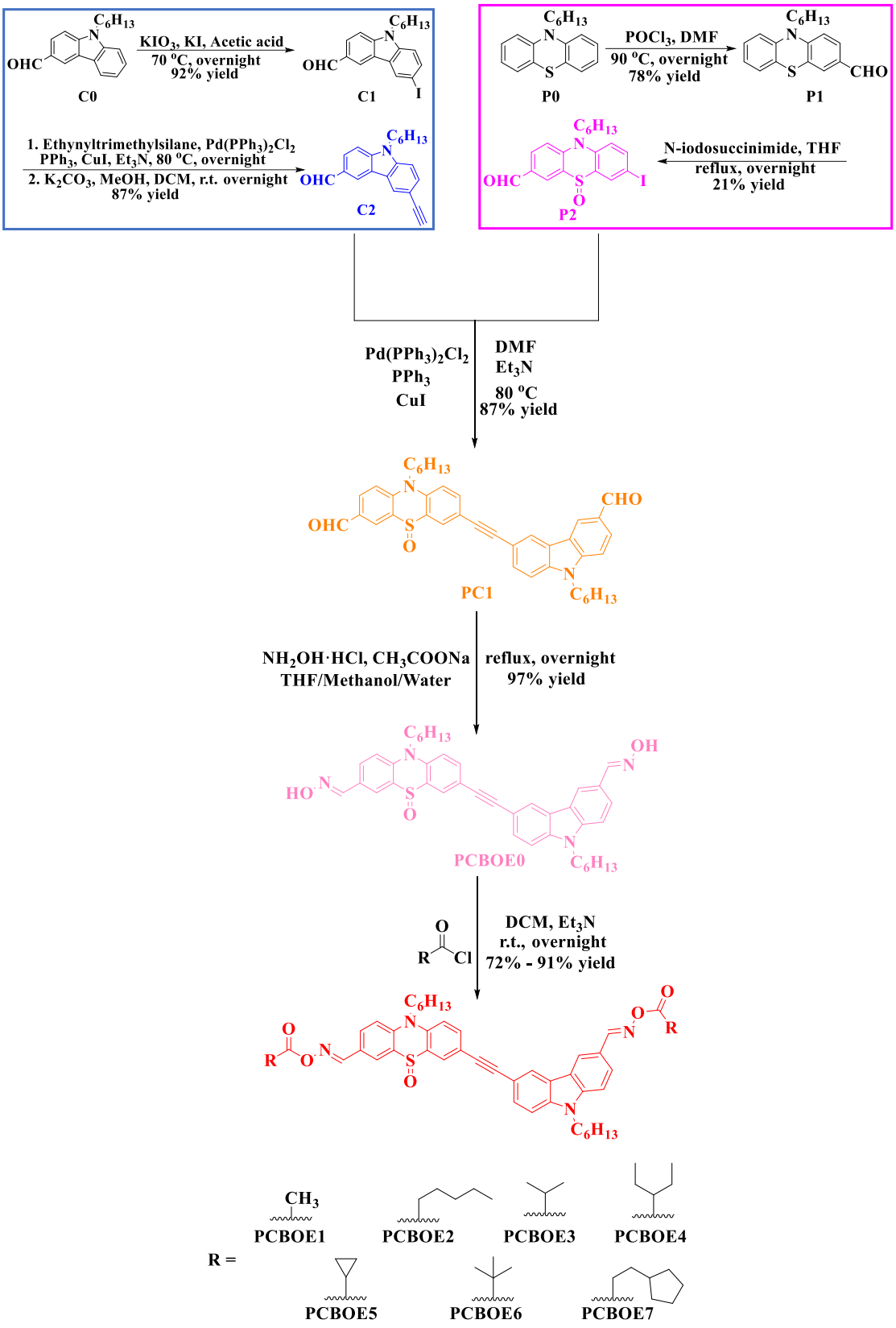

Scheme 4. Synthetic routes of PCBOEs

2.2 Light absorption properties

Figure 1 illustrates the UV-visible absorption spectra of PCBOEs dissolved in THF at a concentration of 2×10^{-5} M in the 300-500 nm range. Table 1 presents the maximum absorption wavelengths (λ_{max}) and molar extinction coefficients (ε) at λ_{max} and 405 nm for PCBOEs. All PCBOEs exhibited an excellent solubility in THF and this excellent solubility can be assigned to the presence of the triple bond. As depicted in Figure 1, PCBOEs displayed a broad absorption band extending up 450 nm. Compared to PCBOE0 for which an absorption maximum located at 353 nm could be determined, PCBOE1-PCBOE7 showed slightly redshifted absorption maxima, ranging between 360 nm and 363 nm. This slight redshift can be assigned to a weak electron-donating effect originating from the oxime ester group.

Table 1 reveals that PCBOE1, PCBOE3, PCBOE4, PCBOE5 and PCBOE6 display higher ε_{max} (ε_{max} = 37500, 40200, 38700, 39000 and 38100 $M^{-1}\cdot cm^{-1}$) compared to PCBOE0 (ε_{max} = 37000 $M^{-1}\cdot cm^{-1}$). This indicates their excellent absorption properties, favorable to photon absorption during photoexcitation. PCBOE2 and PCBOE7 exhibited lower ε_{max} (35300 and 29100 $M^{-1}.cm^{-1}$). Similarly, at 405 nm, PCBOE1, PCBOE3, PCBOE4, PCBOE5 and PCBOE6 demonstrated higher molar extinction coefficients ($\varepsilon_{405\ nm}$ = 4800, 6600, 6200, 8000 and 6000 $M^{-1}\cdot cm^{-1}$) than PCBOE0 ($\varepsilon_{405\ nm}$ = 4500 $M^{-1}\cdot cm^{-1}$), while PCBOE2 and PCBOE7 exhibited lower $\varepsilon_{405\ nm}$. In summary, PCBOEs exhibit a UV-A centered absorption. However, these structures possess sufficient absorption properties in the near-UV/visible range, suggesting their suitabilities as candidates for acrylate polymerization under 405 nm LED irradiation.

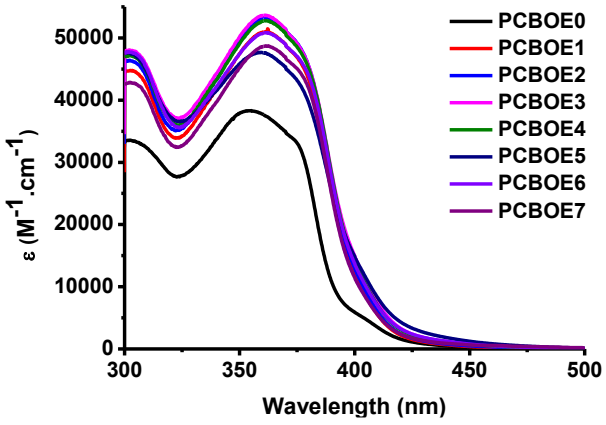

Figure 1. UV-visible absorption spectra of PCBOEs in THF

Table 1. Light absorption properties of PCBOEs in THF

PCBOEs	λ_{max} (nm)	ε_{max} ($M^{-1} \cdot cm^{-1}$)	$\varepsilon_{405\ nm}$ ($M^{-1} \cdot cm^{-1}$)
PCBOE0	355	38300	4700
PCBOE1	362	52500	8400
PCBOE2	361	53300	9100
PCBOE3	361	53700	11000
PCBOE4	361	52800	10200
PCBOE5	361	47600	11400
PCBOE6	361	50800	10000
PCBOE7	361	48700	8100

2.3 Cleavage of the N-O bond

In order to further investigate the chemical changes of PCBOEs dissolved in THF after exposure to a 405 nm LED light source at intensity of 110 $mW \cdot cm^{-2}$, the absorption changes between 300 and 500 nm were examined for PCBOEs irradiated for 0, 60, 120, 180, 240 and 300 s, as shown in Figure 2 and S1. As depicted in Figure 2, compared to PCBOE0, all other PCBOEs containing oxime ester groups exhibited a similar photolysis pattern. Specifically, after 60 s of exposure to 405 nm LED irradiation, there was a significant decrease in absorption values and the λ_{max} exhibited a blue shift of 10 nm. Further extension of the radiation time resulted in minimal changes in the decrease in absorption values and the maximum absorption wavelengths. This compellingly demonstrates the effective cleavage of the oxime ester moieties present in PCBOE1-PCBOE7 after exposure to light.

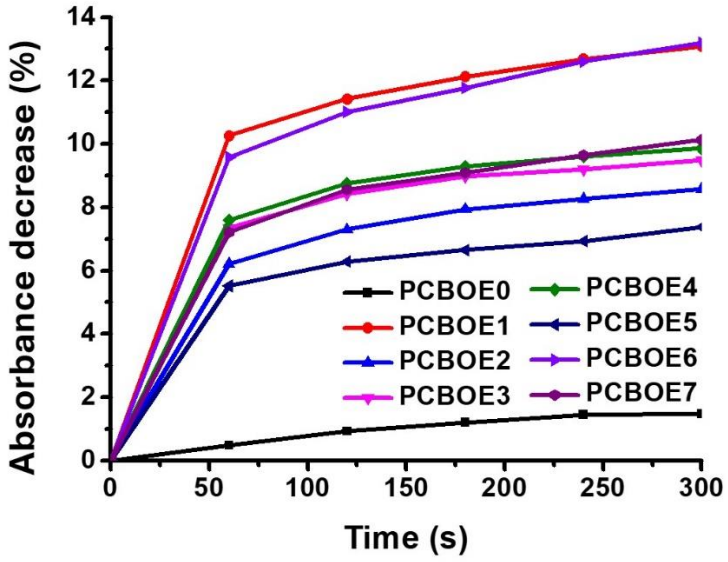

Figure 2. Dye consumption of PCBOEs in THF upon irradiation with 405 nm LED

To analyze the aforementioned photolysis processes from the perspective of energy changes, position of the excited singlet state could be determined from the crossing point between the absorption and emission curves but also from the measurements of the fluorescence decay curves of PCBOEs dissolved in THF. The results are shown in Figure S2, respectively. Table 2 lists the singlet state energy (E_{S1}), triplet state energy (E_T) and N-O bond dissociation energy (N-O BDE). As shown in Table 2, among all PCBOEs, the N-O BDE of PCBOEs containing oxime ester structures are lower than that of PCBOE0. Moreover, the N-O BDE of oxime ester groups connected to carbazole or phenothiazine are similar. Additionally, E_{S1} of all PCBOEs is greater than their N-O BDE, indicating that the cleavage from S_1 can be energetically favorable. Additionally, except for PCBOE0, E_T of all oxime ester-containing PCBOEs are also higher than their N-O BDE, suggesting that the triplet state, reached through intersystem crossing (ISC), can also promote the N-O bond cleavage. It is noteworthy that the fluorescence lifetimes of PCBOEs range from 1.47 to 2.76 ns. Compared to the fluorescence lifetimes of visible light OXEs reported in the literature (See Table S1), the fluorescence lifetimes of PCBOEs are comparable to that determined for different coumarin derivatives exhibiting excellent photoinitiating properties. However, the excited state lifetimes of PCBOEs are shorter than those determined for phenothiazine derivatives (around 4-5 ns) or a *bis*-carbazole derivative

(3.2 ns). Despites longer excited state lifetimes, phenothiazine and *bis*-carbazole derivatives could furnish monomer conversions on par or outperforming benchmark photoinitiators. Overall, PCBOEs exhibit excited state lifetimes comparable to that determined for oxime esters reported in the literature. These short excited state lifetimes can be in agreement with a cleavage from S1. In summary, these positive results indicate that PCBOEs, when excited by an appropriate light source, can undergo a photocleavage of the N-O bond cleavage from the excited states

Table 2. N-O BDE, E_{S1}, E_T, $\Delta H_{Cleavage\ S1}$, $\Delta H_{Cleavage\ T1}$ (kcal · mol^{-1}) and lifetimes (ns) of PCBOEs

CCOBOEs	N-O BDE	E_{S1}	$\Delta H_{Cleavage\ S1}$	E_T	$\Delta H_{Cleavage\ T1}$	Lifetimes
PCBOE0	65.1[a] 64.7[b]	72.1	-7.0 -7.4[b]	56.6	8.5[a] 8.1[b]	1.59
PCBOE1	54.1[a] 54.2[b]	71.5	-17.4[a] -17.3[b]	55.3	-1.2[a] -1.1[b]	1.47
PCBOE2	43.1[a] 42.2[b]	71.3	-28.2[a] -29.1[b]	56.5	-13.4[a] -14.3[b]	1.70
PCBOE3	43.7[a] 43.9[b]	71.1	-27.4[a] -27.2[b]	55.3	-11.6[a] -11.4[b]	1.92
PCBOE4	45.4[a] 45.5[b]	71.2	-25.8[a] -25.7[b]	56.5	-11.1[a] -11.0[b]	1.87
PCBOE5	47.4[a] 47.5[b]	71.2	-23.8[a] -23.7[b]	55.4	-8.0[a] -7.9[b]	2.76
PCBOE6	42.7[a] 42.9[b]	71.4	-28.7[a] -28.5[b]	55.2	-12.5[a] -12.3[b]	1.97
PCBOE7	49.0[a] 47.1[b]	71.7	-22.7[a] -24.6[b]	56.6	-7.6[a] -9.5[b]	1.60

a: oxime ester groups connected to the phenothiazine group;

b: oxime ester groups connected to the carbazole group.

2.4 **Free radical photopolymerization**

Combining the remarkable absorption properties of PCBOEs at 405 nm and their rapid photolysis reactions, photopolymerization efficiencies of PCBOEs (1×10^{-5} mol · g^{-1} and 2×10^{-5} mol · g^{-1}) in TMPTA under 405 nm LED radiation were explored, as shown in Figure 3. Table 3 lists the final acrylate conversions of the PCBOEs/TMPTA systems after 300 s of irradiation. As depicted in Figure 3, irrespective of the concentration in TMPTA, PCBOE0 failed to initiate any TMPTA polymerization after exposure to a 405 nm light source. These results are consistent with its structural specificities, namely this is an oxime and not an oxime ester. This structure is not designed for radical generation. In contrast, PCBOE1-PCBOE7 exhibited promising photopolymerization kinetics. At a concentration of 1×10^{-5} mol · g^{-1}, the lowest final conversion for the PCBOE7/TMPTA system was 59%, PCBOE6 initiated TMPTA polymerization with a conversion rate of 78%, while the final conversions for other PCBOEs fluctuated between 67% and 71%. When the concentration of PCBOEs in TMPTA was increased to 2×10^{-5} mol · g^{-1}, the final monomer conversions with PCBOE1, PCBOE2, PCBOE5 and PCBOE7 increased, consistent with more initiating radicals formed. Among them, PCBOE1 and PCBOE7 exhibited the highest improvements, increasing from 67% to 79% and from 59% to 71%, respectively. This is related to the content and activity of radicals generated after photocleavage. It is worth noting that, although the concentrations of PCBOE3, PCBOE4 and PCBOE6 were increased, the color of the PCBOEs/TPMTA systems became darker, preventing light from penetrating the mixture completely. This indicates that the increase of the photoinitiator concentration is not possible with all oxime esters, due to an inner filter effect adversely affecting light penetration and thus radical generation. Consequently, final monomer conversions did not increase accordingly. In conclusion, PCBOE1, PCBOE2 and PCBOE5 at a concentration of 2×10^{-5} mol · g^{-1} demonstrated positive final conversions in TMPTA after 300 s of 405 nm LED radiation, reaching 79%, 76% and 77%, respectively.

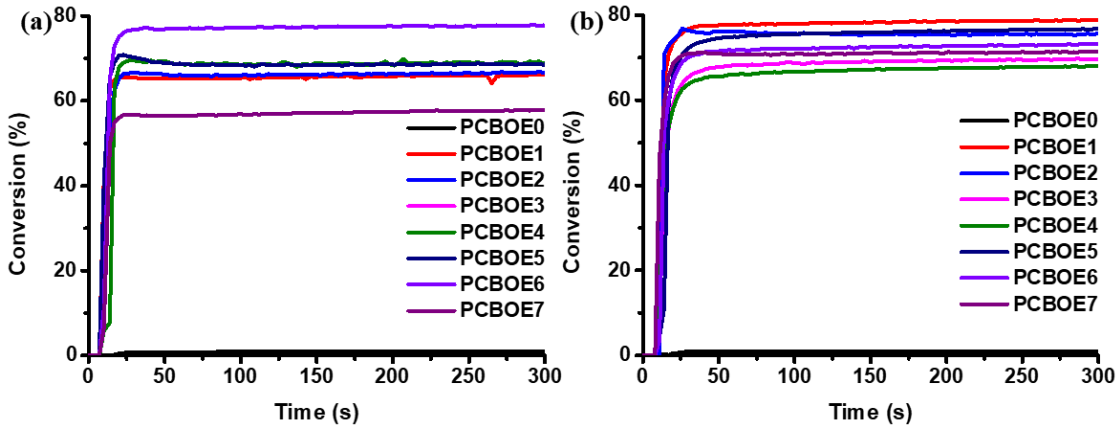

Figure 3. Photopolymerization profiles of TMPTA in laminate (25 μm) upon exposure to a 405 nm LED in the presence of different PCBOEs with concentration of 1×10^{-5} mol · g^{-1} (a), 2×10^{-5} mol · g^{-1} (b) in TMPTA. The irradiation starts at t = 10 s.

Table 3. Final acrylate function conversions (FCs) of TMPTA containing different PCBOEs

PCBOEs	25 μm @405 nm LED 1×10^{-5} mol · g^{-1} Final conversions (FCs, %)	25 μm @405 nm LED 2×10^{-5} mol · g^{-1} Final conversions (FCs, %)
PCBOE0	< 1%	< 1%
PCBOE1	67	79
PCBOE2	71	76
PCBOE3	71	70
PCBOE4	70	68
PCBOE5	71	77
PCBOE6	78	73
PCBOE7	59	71

2.5 Proposed chemical mechanism

Building upon the positive experimental results, a mechanism for the initiation of the TMPTA photopolymerization by PCBOEs after exposure to a specific light source is proposed, as illustrated in Scheme 5. Following excitation by a 405 nm LED irradiation, PCBOEs transition from the ground state to the excited state. Due to the higher singlet and triplet state energies of PCBOEs in this unstable state compared to

the bond dissociation energy of the N-O bond, the N-O bond in PCBOEs readily undergoes a homolytic cleavage, leading to phenothiazine-carbazole iminyl radical and acyloxyl radical. The unstable acyloxy group further undergoes decomposition, releasing carbon dioxide and ultimately generating R• radicals capable of initiating the polymerization of acrylate monomers. The two N-O cleavages certainly occur successively and not concomitantly due to differences of N-O bond energies for the two groups.

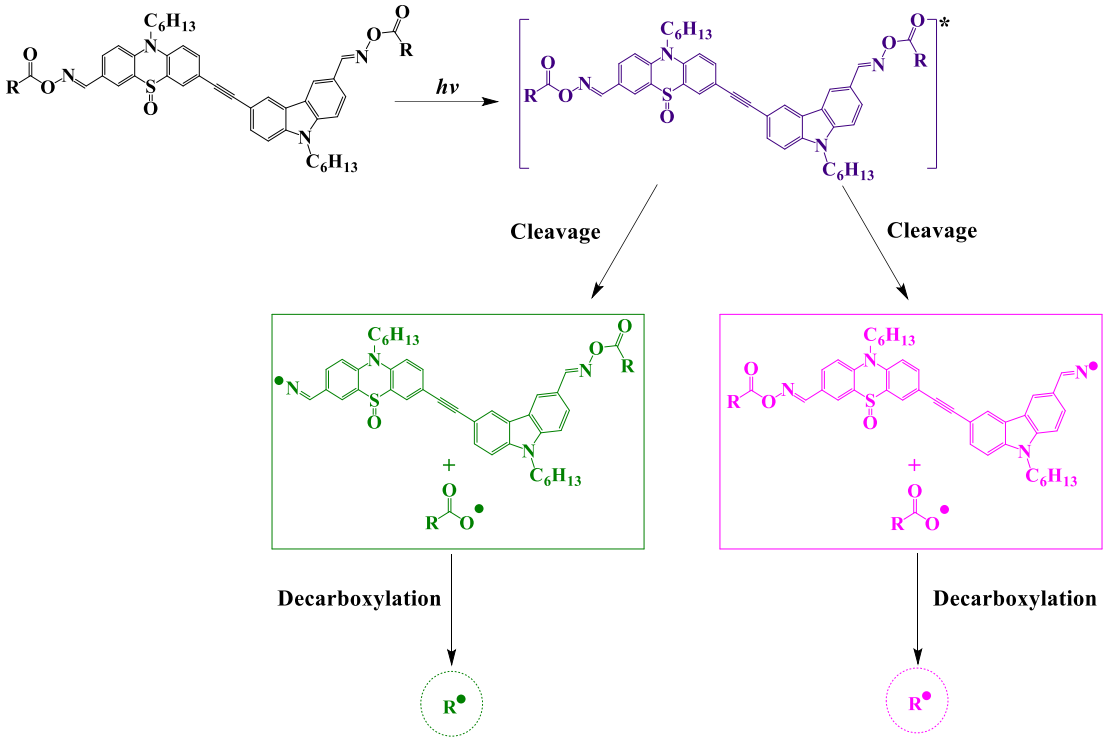

Scheme 5. Proposed chemical mechanism of PCBOE1-PCBOE7

To verify whether the proposed mechanism of PCBOEs generating free radicals is correct, FTIR was first used to confirm that the PCBOEs/TMPTA system produces CO_2 when exposed to a 405 nm LED light. Following this, FTIR was utilized to determine whether the acyloxyl radicals generated after PCBOEs cleavage can undergo a decarboxylation reaction. Figures S3 and S4 display the infrared spectra of PCBOEs (1×10^{-5} mol · g^{-1} and 2×10^{-5} mol · g^{-1}) in TMPTA after 0, 30 and 60 s of 405 nm LED exposure. Contrarily to the PCBOE0/TMPTA system for which no CO_2 release was detected, the CO_2 absorption peaks (2337 cm^{-1}) in the PCBOE1-PCBOE7/TMPTA systems were clearly detected and the intensity of the CO_2 absorption peak increased with time. This positive result strongly corroborates the decarboxylation reaction of

PCBOEs after exposure to 405 nm LED.

Additionally, ESR experiments can be utilized to confirm the aforementioned hypothesis. PCBOE1 and PCBOE6, dissolved in *tert*-butylbenzene, were subjected to 30 s of 405 nm LED irradiation, and the free radical trapping agent *N*-tert-butyl-α-phenylnitrone (PBN) was employed to detect the generation of free radicals. As depicted in Figure 4, methyl radicals were detected in the PCBOE1/*tert*-butylbenzene solution, with calculated hyperfine coupling constants α_N and α_H of 14.6 G and 3.6 G, respectively. Acetoxy radicals were similarly detected, with α_N and α_H of 13.5 G and 1.7 G.[21, 33] In the PCBOE6/*tert*-butylbenzene solution, *tert*-butyl radicals were detected, with calculated hyperfine coupling constants α_N and α_H of 14.4 G and 2.0 G. Acetoxy radicals were also detected, with α_N and α_H of 13.6 G and 1.8 G.[34, 35] Hence, the proposed mechanism of PCBOEs generating free radicals is fully validated.

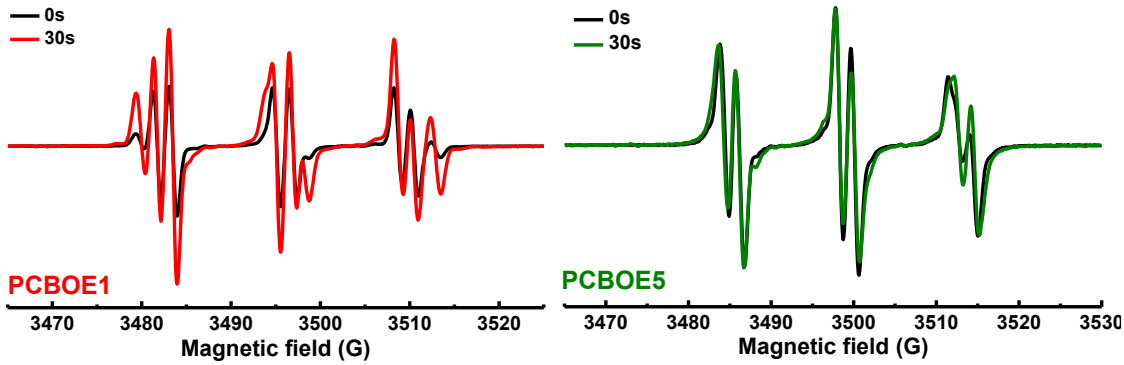

Figure 4. ESR-ST spectra of the PBN radical adducts of PCBOE1 and PCBOE6 under LED@405 nm irradiation in *tert*-butylbenzene

2.6 DLW

To verify the suitability of PCBOEs for additive manufacturing, the PCBOE3 (1×10^{-5} mol · g^{-1})/TMPTA system was selected for 3D printing of a designed pattern using DLW. As shown in Figure 5, an "IS2M" pattern with a height of 1800 μm was successfully fabricated under 405 nm laser diode irradiation. The pattern exhibited very clear contours and a smooth surface with extremely high precision and spatial resolution, as observed through numerical optical microscopy. Therefore, the PCBOE3/TMPTA system demonstrates significant potential for market applications.

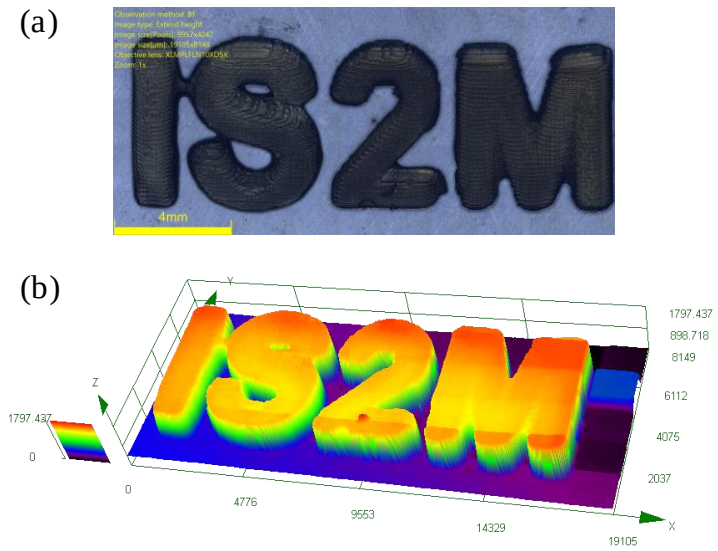

Figure 5. DLW printing patterns (a) and characterization by numerical optical microscopy (b)

2.7 Thermal polymerization

OXEs can also undergo a thermal cleavage when heated at the appropriate temperature and thus generate radicals to initiate the polymerization of acrylate monomers.[20] Therefore, PCBOE0, PCBOE1, PCBOE2 and PCBOE5 (2×10^{-5} mol · g^{-1}) /TMPTA systems were selected to investigate their thermal initiation behaviors using DSC, with the temperature continuously rising from room temperature to 250 °C, as shown in Figure 6. The initial initiation temperature $T_{initial}$, maximum decomposition temperature T_{max} and final conversions are listed in Table S2. As depicted in Figure 6, PCBOE0/TMPTA exhibited the lowest initial decomposition temperature, only at 43 °C. The subsequent PCBOE1/TMPTA had an initial decomposition temperature of 55 °C, while PCBOE2/TMPTA reached a maximum of 65 °C. Meanwhile, the PCBOE1/TMPTA system exhibits the lowest T_{max} at 108 ºC, followed by the PCBOE5/TMPTA system with T_{max} at 123 ºC, the highest maximum temperature was achieved with the PCBOE2/TMPTA system. Considering that primary, secondary (linear or cyclic) radicals are formed upon thermal cleavage and decarboxylation, the linear secondary radicals furnished to the most exothermic reaction. In summary, PCBOEs demonstrated the advantage of initiating TMPTA polymerization at low temperatures. Excitingly, compared to the final conversion of 15% for PCBOE0/TMPTA, other oxime-containing PCBOEs showed a significant

improvement of the final monomer conversion. PCBOE1/TMPTA, PCBOE2/TMPTA and PCBOE5/TMPTA achieved final conversions of 50%, 46% and 55%, respectively.

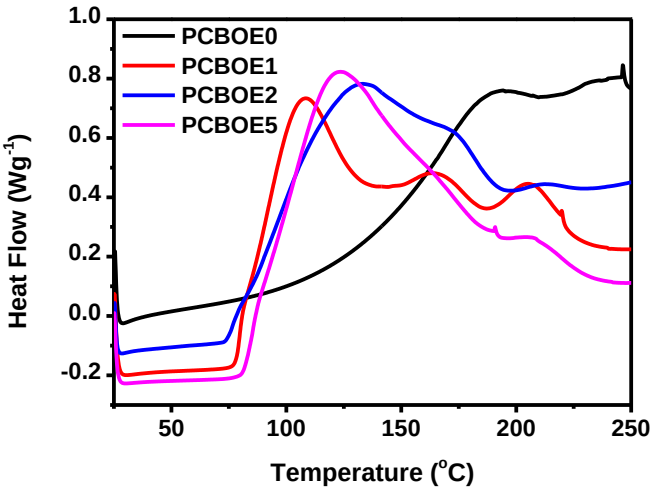

Figure 6. DSC curves of PCBOE0/TMPTA, PCBOE1/TMPTA, PCBOE2/TMPTA and PCBOE5/TMPTA systems

3. Conclusion

In this study, seven PCBOEs, incorporating phenothiazine, carbazole, and two oxime ester groups per molecule, were proposed and successfully synthesized for the first time. Their structures were confirmed by NMR and HRMS. These compounds exhibited a strong absorption in the visible light range and demonstrated excellent photolytic performance under 405 nm LED irradiation, consistent with their photopolymerization abilities in TMPTA. Energy analysis confirmed the theoretical feasibility of the N-O bond cleavage within the PCBOE structures. Possible cleavage and decarboxylation mechanisms were proposed and validated by ESR experiments and CO_2 detection tests. Additionally, the PCBOE3/TMPTA system exhibited a high precision and resolution in DLW experiments. Besides their efficient photoinduced effects, PCBOEs also showed high thermal initiation polymerization efficiencies, indicating a significant commercial potential. In the future, leveraging the multiple reactive sites present in phenothiazine and carbazole, other types of phenothiazine-carbazole-based Type I photoinitiators, such as glyoxylates, acyl phosphine oxides, and α-diketones, could be developed.

Acknowledgments

The authors thank the fundings provided by the ANR PhotoFlat and the Chinese Scholarship Council (CSC). The molecular modelling in this work was performed using HPC resources of the Mesocentre of the University of Strasbourg and the HPC resources from GENCI-IDRIS (Grant 2023-AD010812313R2/Jean_Zay.

Conflicts of interest

The manuscript was written through contributions of all authors. All authors have given their approval to the final version of the manuscript.

Notes

The authors declare no competing financial interest. The raw/processed data required to reproduce these findings can be furnished on demand.

References

[1] L.H. Nguyen, M. Straub, M. Gu, Acrylate-based photopolymer for two-photon microfabrication and photonic applications, Advanced Functional Materials. 15(2) (2005) 209-216.
[2] M. Schilling, V. Colvin, L. Dhar, A. Harris, F. Schilling, H. Katz, T. Wysocki, A. Hale, L. Blyler, C. Boyd, Acrylate oligomer-based photopolymers for optical storage applications, Chemistry of materials. 11(2) (1999) 247-254.
[3] M.G. Ramírez, D. Sirvent, M. Morales-Vidal, M. Ortuño, F.J. Martínez-Guardiola, J. Francés, I. Pascual, LED-cured reflection gratings stored in an acrylate-based photopolymer, Polymers. 11(4) (2019) 632.
[4] S. Kumar, V.P. Rao, J. Joseph. Photopolymer Holography: Review and investigations, Asian Journal of Physics. 24 (2015) 1449-1464.
[5] N. Vorzobova, P. Sokolov. Application of photopolymer materials in holographic technologies, Polymers. 11(12) (2019) 2020.
[6] A. Bagheri, J. Jin. Photopolymerization in 3D printing, ACS Applied Polymer Materials. 1(4) (2019) 593-611.
[7] C. Chandler, D.H. Porcincula, M.J. Ford, T.J. Kolibaba, B. Fein-Ashley, J. Brodsky, J.P. Killgore, A. Sellinger, Influence of fluorescent dopants on the vat photopolymerization of acrylate-based plastic scintillators for application in neutron/gamma pulse shape discrimination, Additive manufacturing. 73 (2023) 103688.
[8] R.S.B. Sosa, D.T. Baldos, B.A. Basilia, 4D Printing of shape memory polymers: a concise review of photopolymerized acrylate-based materials, Diffusion Foundations and Materials Applications. 32 (2023) 1-12.
[9] A.B. Kousaalya, Sustainable photo-curable polymers in additive manufacturing arena: a review, Sustainability & Green Polymer Chemistry Volume 1: Green Products and Processes. (2020) 89-98.
[10] H. Lai, X. Peng, L. Li, D. Zhu, P. Xiao, Novel monomers for photopolymer

networks, Progress in Polymer Science. 128 (2022) 101529.
[11] F. Hammoud, A. Hijazi, M. Schmitt, F. Dumur, J. Lalevée, A review on recently proposed oxime ester photoinitiators, European Polymer Journal. 188 (2023) 111901.
[12] Z. Liu, F. Dumur, Recent advances on visible light Coumarin-based oxime esters as initiators of polymerization, European Polymer Journal. 177 (2022) 111449.
[13] F. Dumur, Recent advances on phenothiazine-based oxime esters as visible light photoinitiators of polymerization, European Polymer Journal. 202 (2024) 112597.
[14] F. Dumur, Recent advances on carbazole-based oxime esters as photoinitiators of polymerization, European Polymer Journal. 175 (2022) 111330.
[15] A. Noon, F. Hammoud, B. Graff, T. Hamieh, J. Toufaily, F. Morlet-Savary, M. Schmitt, T.T. Bui, A. Rico, F. Goubard, S. Péralta, F. Dumur, J. Lalevée, Photoinitiation mechanisms of novel phenothiazine-based oxime and oxime esters acting as visible light sensitive Type I and multicomponent photoinitiators, Advanced Materials Technologies. 8(16) (2023) 2300205.
[16] X. Zhang, X. Peng, D. Zhu, Y. Zhang, M. Le Dot, S. Ozen, M. Schmitt, F. Morlet-Savary, P. Xiao, F. Dumur, J. Lalevée, Preparation of nitro-phenothiazine-based oxime esters as dual photo/thermal initiators for 3D printing, Journal of Polymer Science. 62(12) (2024) 2597-2604.
[17] Y. Zhang, F. Morlet-Savary, M. Schmitt, B. Graff, A. Rico, M. Ibrahim-Ouali, F. Dumur, J. Lalevée, Photoinitiation behavior of phenothiazines containing two oxime ester functionalities (OXEs) in free radical photopolymerization and 3D printing application, Dyes and Pigments. 215 (2023) 111202.
[18] F. Dumur, Recent advances on carbazole-based photoinitiators of polymerization, European Polymer Journal. 125 (2020) 109503.
[19] F. Hammoud, N. Giacoletto, M. Nechab, B. Graff, A. Hijazi, F. Dumur, J. Lalevée, 5, 12-Dialkyl-5, 12-dihydroindolo [3, 2-a] carbazole-based oxime-esters for LED photoinitiating systems and application on 3D printing, Macromolecular Materials and Engineering. 307(8) (2022) 2200082.
[20] J. Feng, Y. Zhang, D. Zhu, et al. Study on the photoinitiation mechanism of carbazole-based oxime esters (OXEs) as novel photoinitiators for free radical photopolymerization under near UV/visible-light irradiation exposure and the application of 3D printing. European Polymer Journal. 202 (2024) 112662.
[21] Y. Zhang, Z. Liu, T. Borjigin, B. Graff, F. Morlet-Savary, M. Schmitt, D. Gigmes, F. Dumur, J. Lalevée, Carbazole-fused coumarin based oxime esters (OXEs): efficient photoinitiators for sunlight driven free radical photopolymerization, Green Chemistry. 25(17) (2023) 6881-6891.
[22] P. Hu, W. Qiu, S. Naumov, T. Scherzer, Z. Hu, Q. Chen, W. Knolle, Z. Li, Conjugated bifunctional carbazole-based oxime esters: Efficient and versatile photoinitiators for 3D printing under one-and two-photon excitation, ChemPhotoChem. 4(3) (2020) 224-232.
[23] S. Liu, N. Giacoletto, M. Schmitt, M. Nechab, B. Graff, F. Morlet-Savary, P. Xiao, F. Dumur, J. Lalevee, Effect of decarboxylation on the photoinitiation behavior of nitrocarbazole-based oxime rsters, Macromolecules. 55(7) (2022) 2475-2485.
[24] R. Zhou, X. Sun, R. Mhanna, J.-P. Malval, M. Jin, H. Pan, D. Wan, F. Morlet-

Savary, H. Chaumeil, C. Joyeux, Wavelength-dependent, large-amplitude photoinitiating reactivity within a carbazole-coumarin fused oxime esters series, ACS Applied Polymer Materials. 2(5) (2020) 2077-2085.
[25] H. Lu, Z. Li, Synthesis and structure-activity relationship of N-substituted carbazole oxime ester photoinitiators, Journal of photopolymer science and technology. 34(3) (2021) 307-313.
[26] T. Zhou, X. Ma, W. Han, X. Guo, R. Gu, L. Yu, J. Li, Y. Zhao, T. Wang, D-D-A dyes with phenothiazine-carbazole/triphenylamine as double donors in photopolymerization under 455 nm and 532 nm laser beams, Polymer Chemistry. 7(1759-9954) (2016) 5039-5049.
[27] L.M. Nhari, E.N. Bifari, A.R. Al-Marhabi, F.A. Al-Zahrani, H.A. Al-Ghamdi, S.N. Al-Ghamdi, A.M. Asiri, R.M. El-Shishtawy, Synthesis of novel phenothiazine, phenoxazine and carbazole derivatives via Suzuki-Miyaura reaction, Journal of Organometallic Chemistry. 989 (2023) 122648.
[28] G. Marotta, M.A. Reddy, S.P. Singh, A. Islam, L. Han, F. De Angelis, M. Pastore, M. Chandrasekharam, Novel carbazole-phenothiazine dyads for dye-sensitized solar cells: a combined experimental and theoretical study, ACS Applied Materials & Interfaces. 5(19) (2013) 9635-9647.
[29] D. Wang, S. Gao, Sonogashira coupling in natural product synthesis, Organic Chemistry Frontiers. 1(5) (2014) 556-566.
[30] A. Elangovan, Y. Wang, T. Ho, Sonogashira coupling reaction with diminished homocoupling, Organic Letters. 5(11) (2003) 1841-1844.
[31] K.V. Arundhathi, P. Vaishnavi, T. Aneeja, G. Anilkumar, Copper-catalyzed Sonogashira reactions: advances and perspectives since 2014, RSC advances. 13(7) (2023) 4823-4834.
[32] X. Ma, R. Gu, L. Yu, W. Han, J. Li, X. Li, T. Wang, Conjugated phenothiazine oxime esters as free radical photoinitiators, Polymer Chemistry 8(39) (2017) 6134-6142.
[33] S. Liu, B. Graff, P. Xiao, F. Dumur, J. Lalevée, Nitro-carbazole based oxime esters as dual photo/thermal initiators for 3D printing and composite preparation, Macromolecular Rapid Communications. 42(15) (2021) 2100207.
[34] Y.K. Chen, D.G. Fleming, Y.A. Wang, Theoretical calculations of hyperfine coupling constants for muoniated butyl radicals, The Journal of Physical Chemistry A. 115(13) (2011) 2765-2777.
[35] F. Ucun, S.G. Aydın, Calculated optimized structures and hyperfine coupling constants of some radical adducts of α-phenyl-N-tert-buthyl nitrone in water and benzene solutions, Journal of Organometallic Chemistry. 759 (2014) 27-32.